

## The Depth of Porphyrin in a Membrane and the Membrane's Physical Properties Affect the Photosensitizing Efficiency

Adina Lavi,\* Hana Weitman,\* Robert T. Holmes,<sup>†</sup> Kevin M. Smith,<sup>†</sup> and Benjamin Ehrenberg\*

\*Department of Physics, Bar Ilan University, Ramat Gan 52–900, Israel, <sup>†</sup>Department of Chemistry, Louisiana State University, Baton Rouge, Louisiana 70803-2755 USA

**ABSTRACT** Photosensitized biological processes, as applied in photodynamic therapy, are based on light-triggered generation of molecular singlet oxygen by a membrane-residing sensitizer. Most of the sensitizers currently used are hydrophobic or amphiphilic porphyrins and their analogs. The possible activity of the short-lived singlet oxygen is limited to the time it is diffusing in the membrane, before it emerges into the aqueous environment. In this paper we demonstrate the enhancement of the photosensitization process that is obtained by newly synthesized protoporphyrin derivatives, which insert their tetrapyrrole chromophore deeper into the lipid bilayer of liposomes. The insertion was measured by fluorescence quenching by iodide and the photosensitization efficiency was measured with 9,10-dimethylantracene, a fluorescent chemical target for singlet oxygen. We also show that when the bilayer undergoes a melting phase transition, or when it is fluidized by benzyl alcohol, the sensitization efficiency decreases because of the enhanced diffusion of singlet oxygen. The addition of cholesterol or of dimyristoyl phosphatidylcholine to the bilayer moves the porphyrin deeper into the bilayer; however, the ensuing effect on the sensitization efficiency is different in these two cases. These results could possibly define an additional criterion for the choice and design of hydrophobic, membrane-bound photosensitizers.

### INTRODUCTION

Photosensitization, which uses porphyrins and porphyrin-like chromophores, has become an active research field in recent years. It is the basis of photodynamic therapy (PDT), a modality of treating malignant tumors. This method relies on preferential uptake of the sensitizer molecules by cells of malignant tissues, and on efficient intersystem crossing from the excited singlet state, following light absorption, to the excited triplet state. Deactivation of this state by ubiquitous oxygen leads to the formation of excited singlet oxygen ( $^1\text{O}_2$ ). This species, being a powerful oxidizing agent, causes critical damage to the tissue via apoptosis or necrosis of the cancer cells. During the last two decades various solid tumors (including skin, lung, breast, bladder) were treated by intravenous injection of a derivative of hematoporphyrin (HPD) and illumination with low-intensity light. This technique became a routine clinical protocol in several medical centers in the world, as well as a very intense research area. Some recent reviews are listed here on general properties of porphyrins as sensitizers (Kessel, 1984; Pottier and Truscott, 1986; Dougherty, 1987, 1993; Gomer, 1991; Henderson and Dougherty, 1992; Moan and Berg, 1992; Schuitmaker et al., 1996; Pandey and Zheng, 2000) and on their preclinical and clinical tests (Kennedy and Oswald, 1984; McCaughan, 1987; Lam et al., 1987; Bown, 1990; Li et al., 1990; Castro et al., 1991; North et al.,

1993; Van Hillegersberg et al., 1994; Moretti, 1994; Mulroney et al., 1994; Ben-Hur and Horowitz, 1995).

There is evidence to indicate that with lipophilic sensitizers the locus of action of PDT is the bilayer membrane (Moan et al., 1989; Berg and Moan, 1997). It was found that most of the damage caused by porphyrins in tumor cells, including electric depolarization, increased permeability, membrane rupture and cell lysis, occurred in the plasma and organelle membranes (Malik and Djaldetti, 1980; Kessel, 1984; Boegheim et al., 1988; Specht and Rodgers, 1991; Paardekooper et al., 1992). Furthermore, it was found that the observed electric depolarization, which can be the immediate cause to, or the result of, the cell's death, arises probably from damage to the membrane proteins (Ehrenberg et al., 1993). In addition, the binding of hematoporphyrin or its derivatives to cellular membranes was found to be a prerequisite for their action (Ehrenberg et al. 1985). These observations suggest that the generation of  $^1\text{O}_2$  by lipophilic porphyrins occurs within the bilayer, which is also the site of damage.

Singlet oxygen-mediated photodynamic reactions in membranes are different from those in homogeneous solutions. First, some of the membrane components are also targets for interaction with  $^1\text{O}_2$  (Straight and Spikes, 1985). More important is the fact that  $^1\text{O}_2$  can diffuse rapidly out of the membrane. The intrinsic lifetime of  $^1\text{O}_2$  in lipid bilayers is, in fact, relatively long (13–35  $\mu\text{s}$ ) depending on the type of lipid (Ehrenberg et al., 1998). When a very efficient singlet oxygen trap is located in the membrane, as much as 90% of the singlet oxygen reacts in the bilayer (Dearden, 1986; Hoebeke et al., 1991). Nevertheless, other studies suggest that the apparent singlet oxygen production-yield by several sensitizers is lower in membranes than in homogeneous solutions (Gottfried et al., 1988; Rodgers,

*Submitted August 13, 2001, and accepted for publication January 18, 2002.*

Address reprint requests to Benjamin Ehrenberg, Department of Physics, Bar Ilan University, Ramat Gan 52900, Israel. Tel.: 972-3-5318427; Fax: 972-3-5353298; E-mail: ehren@mail.biu.ac.il.

© 2002 by the Biophysical Society

0006-3495/02/04/2101/10 \$2.00

1988; Kanofsky, 1989; Gorman and Rodgers, 1992; Gross et al., 1993). This discrepancy can be readily resolved by the rapid diffusion of  $^1\text{O}_2$ , which was generated within the membrane environment of liposomes and cells, out of the membrane. According to the Einstein-Smoluchovsky diffusion equation, using an oxygen diffusion coefficient of  $4.7 \cdot 10^{-5} \text{ cm}^2/\text{sec}$  (Fischkoff and Vanderkooi, 1975), the calculated diffusion path-length within  $1 \mu\text{s}$  is  $\sim 100 \text{ nm}$ , i.e., more than 20 times the thickness of the bilayer. Once the singlet oxygen molecule crosses into the aqueous medium, its lifetime becomes very short ( $\sim 4 \mu\text{s}$ ). Thus, the aforementioned apparently low yield of singlet oxygen, normally measured in membranes, is most likely a result of its rapid escape from the bilayer.

Consequently, a new criterion for the choice and design of a new photosensitizer should be considered, in addition to the accepted requirements. One naturally searches for efficient photochemistry, i.e., good quantum yields for intersystem-crossing and energy transfer to oxygen. A cardinal point is the need for an absorption band at long wavelengths to enable deeper light penetration. One also expects to observe good biochemical attributes, namely, good uptake by the cells' membranes, where much of the photodamage occurs *in vivo*. Preferential binding to cancer cells is beneficial, of course, and no toxicity in the dark is required. Considering the diffusion of singlet oxygen in the membrane, one should also add a criterion for improved photodynamic reaction in the membrane: deep vertical localization of the sensitizer in the membrane, which could increase the dwell time of  $^1\text{O}_2$  within the lipid bilayer and increase membrane-localized damage.

In this work we synthesized a new series of protoporphyrin IX (PP3) derivatives, which possess alkyl carboxylate groups of varying length (Fig. 1, *inset*). We show that the depth of membrane penetration by a porphyrin derivative strongly affects the effectiveness of photodynamic oxidative sensitization. We also determined the effect of several membrane parameters, such as lipid additives and temperature, on the location of the sensitizers, and thus on the efficiency of the photodestructive process induced by singlet oxygen. These results can help to find optimal conditions to be used in cellular photosensitized reactions and could be considered in drug design for PDT.

## MATERIALS AND METHODS

### Chemicals

9,10-Dimethylanthracene (DMA), 9-anthracenepropionic acid (APA), PP3 ( $n = 2$  in Fig. 1, *inset*), egg lecithin (phosphatidylcholine, or PC), cholesterol, and dimyristoyl phosphatidylcholine (DMPC) were obtained from Sigma (St. Louis, MO). 1,6-Diphenyl-hexatriene (DPH) and benzyl alcohol were from Aldrich (Milwaukee, WI); KI was from Merck (Merck, Darmstadt, Germany); and  $\text{Na}_2\text{S}_2\text{O}_3$  was from Frutarom (Haifa, Israel). The other three protoporphyrin derivatives with different alkyl carboxylate groups ( $n = 1, 4$ , and  $6$ , Fig. 1) were synthesized for this project. These

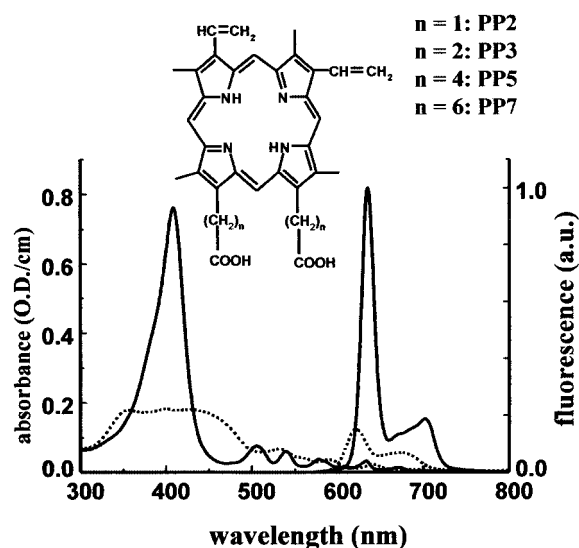


FIGURE 1 Absorption and fluorescence [ $\lambda_{\text{exc}} = 408 \text{ nm}$ ] spectra of  $20 \mu\text{M}$  protoporphyrin-IX (PP3) in water (-----) and in a suspension of lecithin liposomes (—),  $1 \text{ mg/ml}$  (the molar ratio of lipid:dye was 75:1. *Inset*: Chemical structure of PP3 and its modified analogs

syntheses were accomplished from monopyrroles using the *a,c*-biladiene route (Smith, 2000). 2-Formyl-3,5-dimethylpyrroles bearing 4-ester side-chains with different numbers of methylenes ( $n = 1, 4, 6$ ) in the chain were individually reacted with the same dipyrromethane to afford the corresponding *a,c*-biladiene salts; these were then cyclized using the copper(II) oxidation procedure (Smith, 2000). Full experimental details of the syntheses are available (Holmes, 1997).

We prepared stock solutions as follows: the anthracenes and the porphyrins were  $2 \text{ mM}$  in dimethylformamide, KI was  $8 \text{ M}$  in water,  $\text{Na}_2\text{S}_2\text{O}_3$  was  $0.1 \text{ M}$  in water, DPH was  $1 \text{ mM}$  in ethanol.

### Preparations of liposomes

The methanol:chloroform solvent from the lipid stock was evaporated and the lipid was layered at the bottom of a tube. This layer was redissolved in diethyl ether, which was then evaporated. Doubly distilled water was added, the sample was vortexed for 3 min and then sonicated for 20 min by a probe sonicator (MSE, Crawley, UK). To prepare mixed liposomes of lecithin with DMPC or cholesterol, the latter additives were dissolved in the chloroform at the required lipid:additive concentration ratio and the procedure of evaporations and sonication was carried out as described above.

DPH and benzyl alcohol were added to the final liposomes' suspension from their concentrated stock solution so that the volume fraction of the organic solvent in the aqueous suspension did not exceed 1%. DPH was incubated in the liposomes' samples for 1 h. The sensitizers were added from their stock solutions in dimethylformamide and were incubated in the dark for 48 h to reach full binding equilibrium. The need for this incubation time will be discussed in the Discussion section. For fluorescence quenching experiments, KI was added to the suspension of porphyrin-containing liposomes, which also contained  $\text{Na}_2\text{S}_2\text{O}_3$  ( $10^{-5} \text{ M}$ ), to prevent the production of colored  $\text{I}_2$  by oxidation of  $\text{I}^-$ .

### Spectroscopic measurements

Fluorescence intensity, excitation and emission spectra, anisotropy and fluorescence time-drives were all measured on a Perkin-Elmer digital

fluorimeter (model LS-50B, Perkin-Elmer, Norwalk, CT) which is equipped with a polarizer accessory and is PC-controlled. Absorption spectra were measured on a Perkin-Elmer Lambda-9 PC-controlled spectrophotometer. The cuvette holders were temperature-controlled by a refrigerated bath/circulator (model RTE110, Neslab Instruments, Newington, NH). The temperature in the cuvette was measured before and after every experiment to make sure it was constant throughout the duration of the measurements.

## Photosensitization

We used the 501-nm line of an Ar<sup>+</sup> laser (model Innova 200, Coherent, Palo Alto, CA) as the irradiation source for PP3 and its derivatives. The laser beam was transferred to the top of the sample cuvette in the fluorimeter with an optical fiber (Fiberguide Industries, Stirling, NJ), core diameter 400  $\mu$ m. The laser beam transversed the sample cuvette along the long axis, at 90° to the direction of the excitation and emission channels of the fluorimeter. The intensity of the beam near the sample's surface (85–100 mW) was measured with a laser power meter (model PD2-A, Ophir, Jerusalem, Israel), before and after the measurements, to ensure that the power remained constant during the measurement. The ion laser did not exhibit any long-term drift. The sample was air-saturated and stirred magnetically to obtain uniform irradiation of the whole sample.

The attributes of the samples for the photophysical measurements were as follows. The volume of the irradiated sample was 3 ml. The phospholipid concentration in the samples was 1 mg/ml. The photosensitizer was incubated in the suspension for 48 h for full equilibration. The singlet-oxygen target, DMA or APA, was added to the liposomes' suspension, to a 5- $\mu$ M concentration, at least 10 min before measurement. This period is sufficient to reach binding equilibrium. The DMA or APA fluorescence was excited near 360 nm, at a wavelength where the absorbance was <0.05 optical density units. Under such conditions, the fluorescence intensity, monitored at 455 nm, is proportional to the concentration. The target's fluorescence, which is monitored in a time-drive mode, can thus be considered to reflect its disappearance with time because of the photosensitization reaction. The fluorescence monitoring of the target, under these conditions, was done while the sample was illuminated by the laser, *in situ*, as described in the previous paragraph. The fluorimeter has a pulsed light source and phase-sensitive detection electronics. These properties are important as they serve to reject any stray light from the CW laser beam. The fluorescence traces were then fitted to exponential decays by least-squares fitting programs (Origin, Microcal Software, Northampton, MA).

## RESULTS

### Basic properties of the protoporphyrin derivatives

In this study we aimed to probe the effect of the vertical location of a sensitizer in a lipid bilayer on the photosensitizing efficiency. We chose the core structure of PP3 as the sensitizer for this work, firstly, because of its definite structure, as opposed to Photofrin-II or HPD, which are used in clinical tests, but are mixtures of several monomeric and polymeric derivatives of hematoporphyrin. In addition, the nonsymmetrical substituent groups that are attached to the tetrapyrrole ring render the molecule directionally amphiphilic. Namely, the two hydrophobic CH<sub>2</sub>=CH– groups on one side of the molecule should pull that end of the molecule toward the depth of the bilayer, whereas the two charged carboxylates at the end of the alkyl chains should help anchor that part of the molecule at the aqueous inter-

face. Several previous studies showed that many molecules with charged moieties anchor themselves in the membrane with the charged group at the lipid/water interface (Chattopadhyay and London, 1987; Abrams and London, 1993; Kachel et al., 1995).

Fig. 1 shows the absorbance and fluorescence emission spectra of PP3 in water and in a liposome suspension. As can be seen from the absorption spectrum in liposomes, PP3 has a shallow Soret absorption band in the 300- to 500-nm region, and a series of weaker Q bands, which appear as shoulders in the visible region. PP3 is highly aggregated in water (Brown et al., 1976); this causes the lowering of the extinction coefficient and broadening of the Soret band. The absorption spectra of PP2, PP5, and PP7 are identical to the spectrum of PP3. The fluorescence spectrum of PP3 in water exhibits a main band at 621.5 nm and a secondary band at 674 nm. The emission intensity is weak and arises from nonquenched monomers in the mixture.

In lecithin liposomes' suspension, as in organic solvents, the absorption and emission bands sharpen, because of monomerization of the dye in the nonpolar lipid environment. The fluorescence peaks are red-shifted to 635 nm and 702 nm. This bathochromic shift is very common with porphyrins (Kessel and Rossi, 1982). The emission spectra of PP2, PP5, and PP7 also had identical peak locations and shapes as PP3. We used these characteristic fluorescence changes as tools for monitoring our protoporphyrins in the membranes.

### Liposome binding constants

To evaluate the binding, or partitioning, constant of the protoporphyrins to lipid vesicles we monitored the fluorescence intensity of the porphyrin,  $F_{\text{obs}}$ , at the peak's wavelength of the membrane-bound species, as a function of added lipid concentration, [lpd]. At equilibrium, the following equation holds (Ehrenberg, 1992; Roslaniec et al., 2000):

$$F_{\text{obs}} = \frac{F_{\text{init}} + F_{\text{comp}}K_b[\text{lpd}]}{1 + K_b[\text{lpd}]}$$

$F_{\text{init}}$  is the fluorescence intensity measured without lipid, and  $F_{\text{comp}}$  is the fluorescence intensity that would be obtained at complete binding. Fitting the experimental data points to this hyperbolic equation by a nonlinear regression routine yields  $K_b$ . The binding constants are listed in Table 1.

### Comparative depth profiles of the protoporphyrin derivatives

We assessed the relative depth of the porphyrins in the membranes by fluorescence quenching with iodide ions (KI). The large iodide ions, which have a low charge/

**TABLE 1** Quantitative data of the protoporphyrins

Porphyrin	$K_b$ ( $\mu\text{g/ml}$ ) <sup>-1*</sup>	$K_{SV}$ ( $\text{M}^{-1}$ ) <sup>†</sup>	$\Phi_\Delta$ <sup>‡</sup>	$\Phi_\Delta$ <sup>§</sup>
PP2	$0.035 \pm 0.008$	4.74	0.54	1.1
PP3	$0.066 \pm 0.026$	1.35	1.00	1.0
PP5	$0.273 \pm 0.060$	0.94	1.22	1.0
PP7	$0.257 \pm 0.015$	0.65	1.33	0.9

\*Binding constant to lecithin liposomes. <sup>†</sup>Stern-Volmer quenching constant of the protoporphyrins' fluorescence by  $\text{I}^-$ . <sup>‡</sup>Effective singlet oxygen quantum yield in membranes, relative to that of natural PP3, measured with DMA as a chemical, membrane-residing target. <sup>§</sup>Singlet oxygen quantum yield in membranes, relative to that of natural protoporphyrin IX (PP3), measured with APA as a chemical target.

volume value, penetrate to some extent into the lipid phase. However, the deeper the tetrapyrrole ring is inserted in the lipid bilayer, the less accessible it will be to the quencher and it will yield a lower Stern-Volmer quenching constant (Ehrenberg and Gross, 1988; Langner and Hui, 1991; Barenholz et al., 1991; Moro et al., 1993; Deumie et al., 1995).

Fig. 2 shows the quenching data obtained for the liposome-bound porphyrins along with the lines that were fitted to the Stern-Volmer equation:

$$F_0/F = 1 + k_q\tau_0[Q] = 1 + k_{SV}[Q] \quad (1)$$

where  $F_0$  is the fluorescence without quencher, and  $F$  is the fluorescence with iodide at concentration  $[Q]$ . The values of the measured quenching constants are shown in Table 1.

### Photosensitization efficiencies

In all singlet oxygen quantum yield experiments, we used DMA or APA as chemical targets of singlet oxygen. DMA was chosen for the following reasons: it has a high reaction rate and specificity with singlet oxygen (Corey and Taylor,

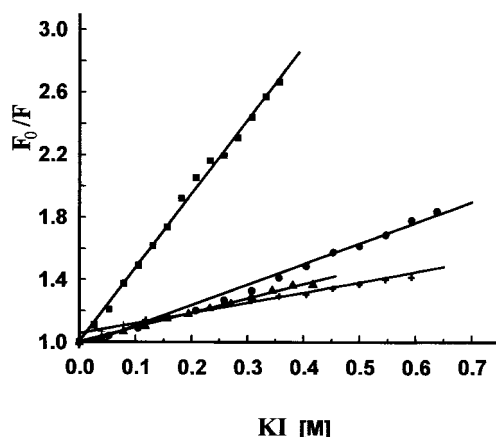


FIGURE 2 Stern-Volmer plots for iodide quenching of the fluorescence of protoporphyrin derivatives in 1 mg/ml lecithin liposomes. ■, PP2; ●, PP3; ▲, PP5; +, PP7.  $\lambda_{exc} = 501$  nm,  $\lambda_{em} = 636$  nm. The solid lines are the least squares linear fits.

1964; Usui, 1973; Wilkinson and Brummer, 1981); it binds efficiently to lipid vesicles (Gross et al., 1993); its fluorescence intensity is greatly enhanced upon binding to lecithin liposomes, which makes it easy to follow and monitor its photosensitized peroxidation in the lipid/environment. The second target, APA, was chosen because its charged carboxylate group would anchor it at the lipid/water interface, as opposed to the nonpolar DMA, which can penetrate freely into the bilayer.

For evaluating the relative singlet oxygen quantum yields we monitored the rate of fluorescence disappearance of DMA (or APA) caused by sensitization of the protoporphyrins. The experimentally observed exponential decay of fluorescence of DMA,  $F$ , is described by:

$$F_{DMA} = F_0 e^{-k_{DMA}t} \quad (2)$$

$$k_{DMA} = \frac{k\Phi_\Delta}{\alpha} \quad (3)$$

where  $\Phi_\Delta$  is the singlet oxygen quantum yield,  $1/\alpha$  is the ratio between the rate constant for the reaction of singlet oxygen with the target and the sum of the rate constants of all the deactivation pathways of singlet oxygen (Wasserman and Murray, 1979), and  $k$  is the rate of photons' absorption by the sensitizer and is given by:

$$k = \frac{0.97 \cdot P \cdot (1 - 10^{-OD})}{(0.1197/\lambda) \cdot V}$$

Here,  $P$  is the power of the laser, in mW; OD is the optical density of the sample at the laser wavelength  $\lambda$ ;  $V$  is the volume of the irradiated sample in milliliters. The factor 0.97 is introduced to correct for the reflection of the laser at the sample/air interface by Fresnel's equations of reflection. Singlet oxygen quantum yields,  $\Phi_\Delta$ , relative to that of natural protoporphyrin (PP3), measured with the two singlet oxygen targets, DMA and APA, are shown in Fig. 3 and in Table 1.

### Effect of membrane fluidization by temperature or benzyl alcohol

We measured the photosensitization efficiency of PP3 in DMPC liposomes, as reflected in the kinetics of photodestruction of the anthracene targets, as a function of temperature. We spanned the range from 10°C where the DMPC bilayer is in the gel phase, up to 40°C, where the lipid bilayer is in the liquid-crystalline phase. The singlet oxygen quantum yields are shown in Fig. 4, relative to the yield at 10°C. This figure also shows the effect of temperature on iodide fluorescence quenching in the same samples.

We also used benzyl alcohol, which is known to fluidize phospholipid membranes (Colley and Metcalfe, 1972; Deckmann et al., 1985), and added it up to 0.6% v:v to the DMPC liposomes. The fluorescence anisotropy of DPH was



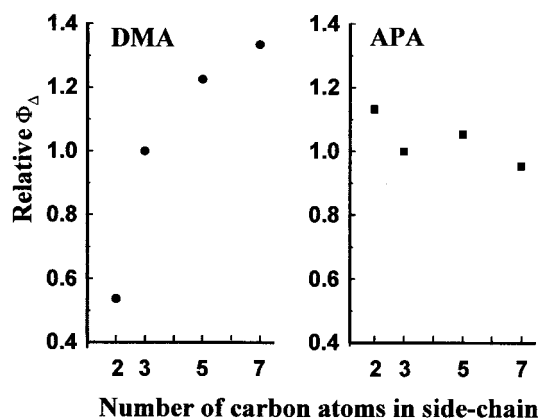


FIGURE 3 Photosensitization reaction efficiencies by the four protoporphyrin derivatives, relative to PP3. The concentration of the protoporphyrins was 2  $\mu$ M, the irradiation source was an Ar<sup>+</sup> laser at 501 nm, the concentration of the target (DMA, *left panel* or APA, *right panel*) was 5  $\mu$ M, its fluorescence was excited at  $\lambda_{\text{exc}} = 360$  nm and measured at  $\lambda_{\text{em}} = 455$  nm.

measured as a function of benzyl alcohol content in DMPC liposomes, and at 20°C it decreased from 0.29 to 0.165, as seen in Fig. 5. Next we measured the relative photosensitization efficiencies by PP3, in DMPC liposomes that contained increasing amounts of benzyl alcohol, at a constant temperature, using DMA as the molecular target. A 50% decrease in the singlet oxygen quantum yields is seen in Fig. 5.

### Effect of cholesterol

Fig. 6 shows the relative singlet oxygen quantum yields of the four protoporphyrins in egg PC vesicles, which contain

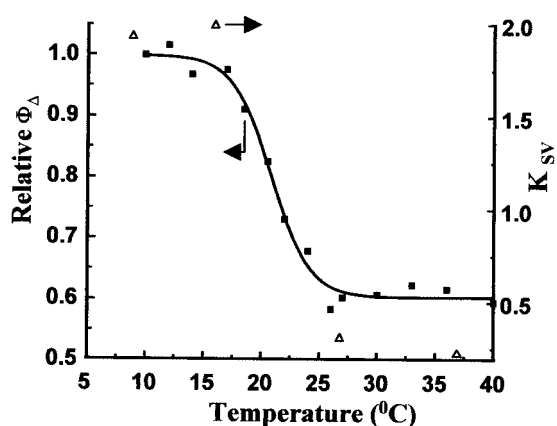


FIGURE 4 Photosensitization efficiencies by PP3 in DMPC liposomes (1 mg/ml) as a function of temperature, relative to that at 10°C (■). The irradiation source, DMA concentration, and the measurement of its fluorescence were as in Fig. 3. The fitted Gaussian titration line is shown. (Δ) Fluorescence quenching constants of PP3 (2  $\mu$ M) by I<sup>-</sup> in DMPC liposomes (1 mg/ml). The fluorescence of PP3 was excited at  $\lambda_{\text{exc}} = 501$  nm, and measured at  $\lambda_{\text{em}} = 636$  nm.

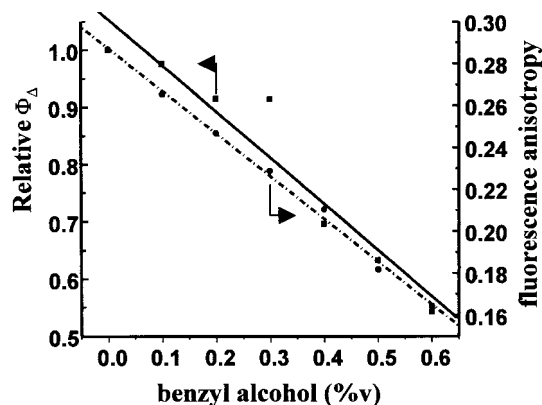


FIGURE 5 Photosensitization efficiencies of PP3, in DMPC liposomes (1 mg/ml) as a function of benzyl alcohol content, relative to the yield at 0% benzyl alcohol (■). Steady state fluorescence anisotropy of DPH (2  $\mu$ M,  $\lambda_{\text{exc}} = 365$  nm,  $\lambda_{\text{em}} = 430$  nm) (●).  $T = 20^\circ\text{C}$ . The irradiation source, DMA concentration, and the measurement of its fluorescence, were as in Fig. 3. The least-squares fitted straight lines are shown.

increasing fractions of cholesterol. This figure demonstrates that adding cholesterol to the membrane lowers the photosensitizing ability of all four sensitizers, although to a different extent. This is manifested in the slopes of the linear curves that were fitted to each set of data. The slope for PP2 ( $-0.023$ ) decreases by almost a factor of five in PP7 ( $-0.005$ ). When the four porphyrins are compared at any concentration of cholesterol in the membrane, the longer-chain molecules are inserted deeper in the bilayer, and should therefore cause greater photodynamic damage. Fig. 7 shows the efficiency of Stern-Volmer quenching of the fluorescence of PP3 upon increasing the cholesterol content in the bilayer.

### Effect of DMPC

DMPC is known to increase the order parameter of a lecithin bilayer membrane and to rigidify it (Cogan et al., 1973; Shinitzky and Inbar, 1976; Van der Meer, 1993), yet it does not act as a chemical or physical quencher of singlet oxygen. Fig. 8 shows the relative quantum yields of PP3 in suspensions of lecithin vesicles, which contain increasing fractions of DMPC. As opposed to cholesterol, raising the amount of DMPC in the membrane enhances the photosensitizing capability. Upon increasing the content of DMPC from 0 to 30%, PP3 exhibits a 3.5-fold gain in its photosensitizing capability. We also measured the relative depth profiles of the protoporphyrins by I<sup>-</sup> quenching and found (Fig. 8) that the addition of DMPC to the lipid does move the sensitizer deeper into the lipid bilayer, where it is less accessible to iodide quenching.

### DISCUSSION

The binding constants of the protoporphyrins are high, as expected from their hydrophobicity, and they increase with

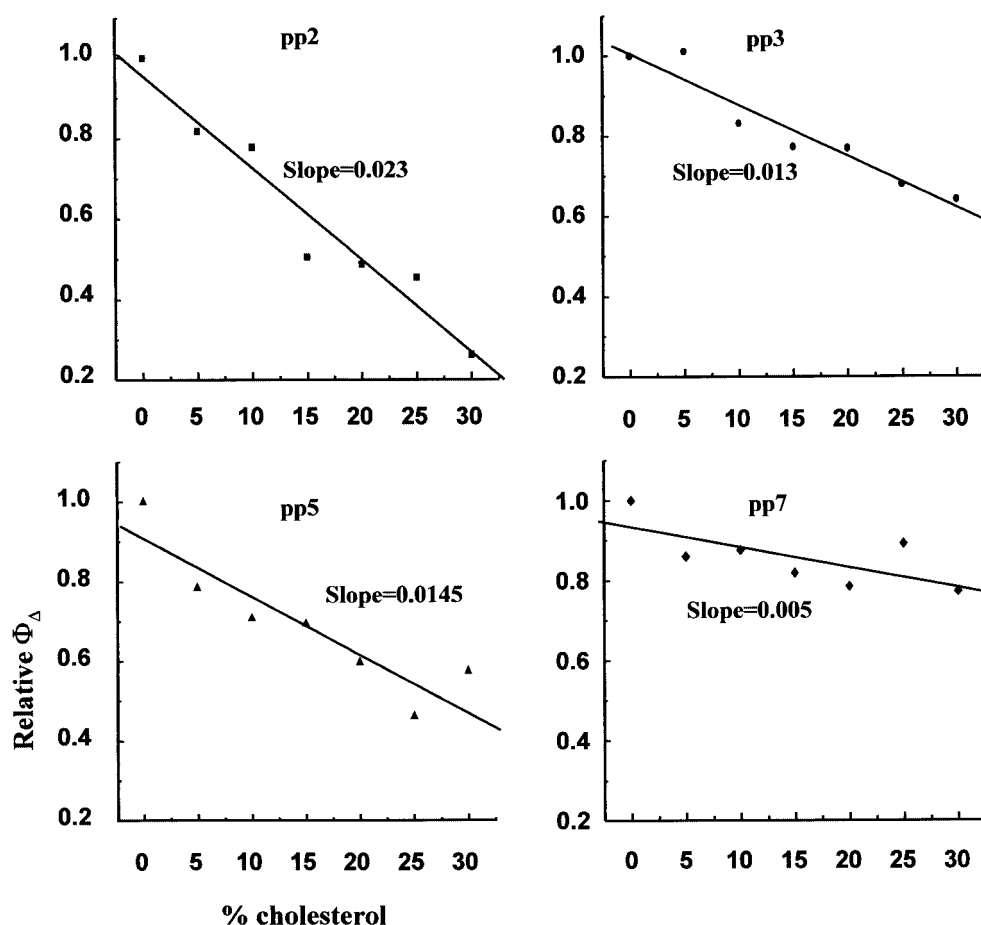


FIGURE 6 Photosensitization efficiencies of the protoporphyrins in lecithin vesicles, which contain increasing fractions of cholesterol. The singlet oxygen yield in each case is relative to that with 0% cholesterol. The irradiation source, DMA concentration, and the measurement of its fluorescence were as in Fig. 3. The arbitrary fitted straight lines and their slopes are shown.

the number of carbon atoms in the carboxylate chain. Even for PP2, with the lowest  $K_b$ ,  $0.035 \pm 0.008 (\mu\text{g/ml})^{-1}$ , 50% binding of the porphyrin is achieved at  $28.6 \mu\text{g lipid/ml}$  (i.e.,  $1/0.035$ ). For PP5,  $K_b$  rises to  $0.273 \pm 0.060 (\mu\text{g/ml})^{-1}$ . In comparison, HPD and Photofrin-II have much lower binding constants,  $0.012$  and  $0.0092 (\mu\text{g/ml})^{-1}$ , respectively (Gross and Ehrenberg, 1989). The difference is probably attributable to the hydrophobicity of the vinyl side groups, compared with the hydroxyl moieties of hematoporphyrin. Elongation of the alkyl carboxylate chains contributes to an increase in the hydrophobicity, which is reflected by a stronger binding constant.

As seen in Fig. 2, the quenching plots yield very good linear fits, with a  $y$  axis intercept of  $\sim 1$ . It proves that the protoporphyrin population is homogeneous, that it is accessible to the iodide ions, and that there are no subpopulations hidden from the quencher. Indeed, attempts to plot the quenching data according to the modified approach to quenching (Lehrer, 1971), that considers fluorophore subpopulations that are not accessible to the quencher, con-

firmed that the quenchable fraction of the protoporphyrins was 1. The quenching results in Table 1 verify that a porphyrin with a longer alkyl carboxylate group is inserted deeper within the lipid bilayer. PP7, the porphyrin with the longest chain, is the most protected and therefore the least accessible to the iodide ions, thus having the lowest quenching constant,  $0.65 \text{ M}^{-1}$ , whereas PP2, which is the closest to liposome/water interface, has the highest quenching constant,  $4.74 \text{ M}^{-1}$ .

A study by Kusaj et al. (1996) showed that when the emission of protoporphyrin was quenched by iodide in the presence of phospholipid vesicles, the Stern-Volmer plots curved downward. Such curvature suggested to the authors the existence of a heterogeneous population of at least two classes of protoporphyrin fluorophores, which possess different quenching constants. Their conclusion was that one fraction of PP is embedded in the lipid phase and is inaccessible to the quencher, and the other fraction, which is accessible to the iodide ion, is localized outside the liposome, with the ionized propionic chains of the porphyrin

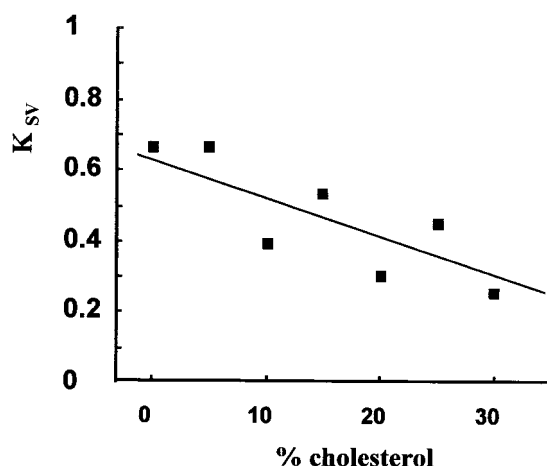


FIGURE 7 Fluorescence quenching constants of PP3 (2  $\mu$ M) by  $I^-$ , in lecithin liposomes that contain increasing amounts of cholesterol. The total lipid concentration was 1 mg/ml. The fluorescence of PP3 was measured as in Fig. 4.

interacting with the polar heads of membrane phospholipids. We think that the explanation to those observations is different. The downward curvature is probably the result of a too-short incubation time (1 h), which was used in the mentioned study. From our binding kinetics curves, we know that after 1 h, a fraction larger than 20% of the protoporphyrin is still in the aqueous phase and is not yet bound to the liposomes. Without vigorous stirring during the incubation, full binding is reached only after >24 h. Thus, after 1 h of incubation there could indeed be two different subpopulations of PP, but it is not an equilibrium state. Our results show that when equilibrium is attained, a

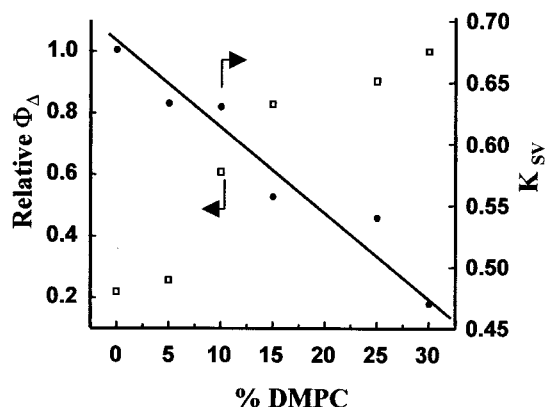


FIGURE 8 (□) Photosensitization efficiency of PP3 in suspensions of egg PC vesicles, which contain increasing ratios of DMPC, relative to 0% DMPC. Total lipid concentration was 1 mg/ml. The irradiation source, DMA concentration and the measurement of its fluorescence were as in Fig. 3. (●) Fluorescence quenching constants of PP3 (2  $\mu$ M), by  $I^-$ , in lecithin liposomes that contain increasing amounts of DMPC. The total lipid concentration was 1 mg/ml. The fluorescence of PP3 was measured as in Fig. 4.

homogeneous population, accessible to iodide ions and fully bound to the liposomes, is indeed obtained.

The important result seen in Fig. 3 is a 2.5-fold increase in the photooxidation efficiency of DMA when the number of carbon atoms in the side chains is increased from 2 to 7. When APA was used, the photooxidizing efficiency seems not to be influenced by the vertical placement of the sensitizer. This difference originates, in our opinion, from the localization of the target in the membrane. APA is probably anchored by its charged carboxylate moiety at, or near, the lipid:water interface. Singlet oxygen, which is generated at different depths within the bilayer, diffuses rapidly through the membrane and much faster than its natural lifetime in DMPC liposomal environment, which was assessed as 36.4  $\mu$ s (Ehrenberg et al., 1998). Thus, singlet oxygen molecules have a chance for chemical interaction with the target when it reaches the liposome/water interface, where the anthracene molecule is localized. Therefore, the probability of singlet oxygen to react with the target depends much less on the depth of its origin. However, when DMA is used, the chances of the latter to react with this delocalized target are greater if the diffusion path of the oxygen originates from a deeper location in the membrane. In this case the extended time that singlet oxygen stays within the membrane increases the photosensitization efficiency. London (Asuncion-Punzalan and London, 1995; Kachel et al., 1995) has indeed demonstrated, by the fluorescence parallax method, the difference in the vertical displacement of methyl-anthracene and anthracene with a polar, or charged, group at the 9 position.

Raising the temperature through the melting phase transition causes a 40% decrease in the sensitization efficiency. The midpoint of the change is calculated from the fitted sigmoidal curve, as  $20.8 \pm 0.3^\circ\text{C}$ . At the same time, the Stern-Volmer quenching constant changes from  $\sim 2 \text{ M}^{-1}$  at temperatures below the phase transition, when the membrane is in the gel state, to  $\sim 0.25 \text{ M}^{-1}$  in the liquid-crystalline state (Fig. 4). A temperature or phase-transition effect on  $I^-$  penetration would be expected to be in an opposite direction to the observed effect. Therefore, the latter results show that fluidizing the membrane by increasing the temperature displaces the sensitizer deeper into the membrane, or rather that in the solid gel state the porphyrin is extruded toward the lipid:water interface. We have to rationalize the deepening of the sensitizer, which emerges from these quenching experiments, with the concomitant decrease of the photosensitizing efficiency upon increasing the temperature. The fact that there is a phase transition proves that the shift in the sensitizer's position is a result of the change in fluidity and not an effect of temperature.

We therefore used another tactic to fluidize the membrane, to check whether there is a coherent trend in the photosensitizing efficiency as a result of membrane fluidity. Fluidization by benzyl alcohol leads to a similar effect as the increase of the temperature. Namely, it facilitates deeper

sinking of the sensitizer in the lipid bilayer, but a corresponding increase of the photosensitizing efficiency is not observed. These apparently contradicting findings are explainable on the basis of oxygen's diffusion in biological and artificial membranes (Fischkoff and Vanderkooi, 1975). These researchers determined oxygen diffusion coefficients in phospholipid dispersions and found a strong increase in oxygen's diffusion constant occurring at the phase transition temperature of liposomes. The authors added that it could not be determined whether the increase in pyrene quenching above the phase transitions of DMPC and DPPC was attributable to increased oxygen solubility or to a rise in the diffusion coefficient; however, the oxygen flux in a membrane in a fluid state was greater than in the solid-gel state. Our results strengthen the assertion that what mainly happens at the phase transition is an increase in oxygen's diffusion coefficient more than an increase in oxygen solubility, as the latter would have resulted in higher photosensitizing quantum yields at increased temperatures because of the higher concentration of oxygen within the lipid bilayer. The lower efficiencies that are obtained because of the fluidity of the membrane can thus be explained as arising from an increase of the diffusion coefficient. The more rapid diffusion of oxygen in the liquid-crystalline state lowers the probability of the photosensitization process.

Addition of cholesterol, above the phase transition temperature, is known to rigidify lipid bilayer membranes (Shinitzky, 1984). Introduction of cholesterol into the membrane causes a broadening of the central low dielectric, hydrophobic, region of the bilayer, by excluding water molecules which penetrate into the bilayer (Shinitzky, 1979; Simon et al., 1982; Zavoico et al., 1985).

Previous studies demonstrated the effect of various lipid additives and of membrane physical parameters on the binding of HPD and Photofrin-II to lipid membranes. Evaluation of the partition of HPD and Photofrin-II into PC and mixed PC/cholesterol liposomes demonstrated that increasing the cholesterol content caused a decrease in both HPD and Photofrin-II association (Gross et al., 1987; Ehrenberg and Gross, 1988). The vertical distribution of these two porphyrins was also affected by a change of the lipid environment. Photofrin-II was found to reside deeper in the membrane than HPD. Cholesterol was also found to modulate the depth profile of both dyes, shifting the two porphyrins closer to the lipid/water interface. However, the effect of DPPC and DMPC on the distribution of the two dyes was not the same. (Ehrenberg and Gross, 1988). The effect of these phosphatidylcholines on HPD was similar to the effect of cholesterol, namely, decreasing the binding to the membrane and shifting the sensitizer toward the aqueous phase. However, with Photofrin-II, adding DMPC or DPPC had an opposite effect; i.e., the binding increased upon rigidization by DPPC and DMPC. In view of these findings, that varying membrane composition affects the vertical distribution and the binding characteristics of the sensitizer, the

measured photosensitizing efficiencies should also be affected by the change.

It is evident from Fig. 7 that addition of cholesterol shields the porphyrin from aqueous  $I^-$  quenching, possibly by sinking it deeper in the membrane. In contrast, the data in Fig. 6 show that addition of cholesterol lowers the photodamage, possibly by extruding the porphyrins toward the lipid/water interface. This apparent decrease in photosensitizing efficiency despite the increase of the singlet oxygen dwell time within the membrane because of deeper insertion can be explained as follows. Cholesterol is an efficient target for  $^1O_2$ . The reaction kinetic rate constant of DMA with singlet oxygen is of the order of  $10^7 \text{ M}^{-1}\text{s}^{-1}$  (Wilkinson et al., 1995) and for cholesterol it is  $\sim 3$  orders of magnitude less (Wilkinson et al., 1995; Straight and Spikes, 1985). However, cholesterol is present in the membrane at a molar concentration that is  $>100$  times higher than DMA, thus it exhibits a significant effect on the consumption of singlet oxygen. As a result, singlet oxygen production efficiency, as measured with DMA, seems to decrease when the additive is cholesterol, even though the sensitizer is located deeper in the bilayer.

Addition of a saturated phospholipid such as DMPC increases the order of the membrane and allows better solubilization of hydrophobic species. Protoporphyrin, which is highly hydrophobic, is moved deeper into the membrane, indicated by the decreased Stern-Volmer quenching (Fig. 8). In turn, this confers the desired effect of an extended dwell time of the singlet oxygen in the membrane and higher photosensitization efficiency (Fig. 8). The results demonstrate that though both cholesterol and DMPC act as rigidifiers of the lipid membrane, they affect the photosensitizing efficiency in different ways. The proper choice of a membrane additive can thus be used to enhance the membrane-localized damage by photodynamic reaction.

In conclusion, this study demonstrates the importance of the vertical localization of a photosensitizer in a lipid membrane on the observed photosensitization efficiency of a membrane-localized target. A new, additional criterion for the choice and design of hydrophobic, membrane-bound photosensitizers emerges here, namely its depth in the membrane. This will have to be tested in each specific use, because the membranes of cells contain additional chemical quenchers of singlet oxygen. We have also demonstrated the important effect of fluidization of the membrane, which is obtained by a fluidizing additive or by increasing the temperature, or of other lipid membrane additives, on the measured photosensitization efficiency.

We acknowledge the support (grant No. 9800364) of the United States-Israel Binational Science Foundation (BSF), Jerusalem, Israel (to B.E.), and National Institutes of Health grant HL-22252 (to K.M.S.). B. Ehrenberg also acknowledges the support of the Michael David Falk Chair in Laser Phototherapy.



## REFERENCES

- Abrams, F. S., and E. London. 1993. Extension of the parallax analysis of membrane penetration depth to the polar region of model membranes—use of fluorescence quenching by a spin-label attached to the phospholipid polar headgroup. *Biochemistry*. 32:10826–10831.
- Asuncion-Punzalan, E., and E. London. 1995. Control of the depth of molecules within membranes by polar groups: determination of the location of anthracene-labeled probes in model membranes by parallax analysis of nitroxide-labeled phospholipid induced fluorescence quenching. *Biochemistry*. 34:11460–11466.
- Barenholz, Y., T. Cohen, R. Korenstein, and M. Ottolenghi. 1991. Organization and dynamics of pyrene and pyrene lipids in intact lipid bilayers. Photo-induced charge transfer processes. *Biophys. J.* 60:110–124.
- Ben-Hur, E., and B. Horowitz. 1995. Advances in photochemical approaches for blood sterilization. *Photochem. Photobiol.* 62:383–388.
- Berg, K., and J. Moan. 1997. Lysosomes and microtubules as targets for photochemotherapy of cancer. *Photochem. Photobiol.* 65:403–409.
- Boegheim, J. P., J. W. M. Lagerberg, T. M. A. R. Dubbelman, K. Tijssen, H. J. Tanke, J. Van der Meulen, and J. Van Steveninck. 1988. Photodynamic effects of HPD on the uptake of rhodamine 123 by mitochondria of intact murine L929 fibroblasts and Chinese hamster ovary K1 cells. *Photochem. Photobiol.* 48:613–620.
- Bown, S. G. 1990. Photodynamic therapy to scientists and clinicians—one world or two? *J. Photochem. Photobiol. B. Biol.* 6:1–12.
- Brown, S. B., M. Shillcock, and P. Jones. 1976. Equilibrium and kinetic studies of the aggregation of porphyrins in aqueous solution. *Biochem. J.* 153:279–285.
- Castro, D. J., R. E. Saxton, R. B. Lufkin, R. P. Haugland, A. A. Zwarun, H. R. Fetterman, J. Soudant, P. H. Ward, and H. Kangaroo. 1991. Future directions of laser phototherapy for diagnosis and treatment of malignancies: fantasy, fallacy, or reality? *Laryngoscope*. 101:1–10.
- Chattopadhyay, A., and E. London. 1987. Parallax method for direct measurement of membrane penetration depth utilizing fluorescence quenching by spin labeled phospholipids. *Biochemistry*. 26:39–45.
- Cogan, U., M. Shinitzky, G. Weber, and T. Nishida. 1973. Microviscosity and order in the hydrocarbon region of phospholipid and phospholipid-cholesterol dispersions determined with fluorescence probes. *Biochemistry*. 12:521–528.
- Colley, C. M., and J. C. Metcalfe. 1972. The localization of small molecules in lipid bilayers. *FEBS Lett.* 24:241–246.
- Corey, E. J., and W. T. Taylor. 1964. A study of the peroxidation of organic compounds by externally generated singlet oxygen molecules. *J. Am. Chem. Soc.* 86:3881–3882.
- Dearden, S. J. 1986. Kinetics of  $O_2 (^1\Delta_g)$  photo-oxidation reactions in egg-yolk lecithin vesicles. *J. Chem. Soc. Faraday Trans. I.* 82: 1627–1635.
- Deckmann, M., R. Haimovitz, and M. Shinitzky. 1985. Selective release of integral proteins from human erythrocyte membranes by hydrostatic pressure. *Biochim. Biophys. Acta.* 821:334–340.
- Deumie, M., M. Elbaraka, and E. Quinones. 1995. Fluorescence quenching of pyrene derivatives by iodide compounds in erythrocyte membranes: an approach of the probe location. *J. Photochem. Photobiol. A. Chem.* 87:105–113.
- Dougherty, T. J. 1987. Photosensitizers: therapy and detection of malignant tumors. *Photochem. Photobiol.* 45:879–889.
- Dougherty, T. J. 1993. Photodynamic therapy. *Photochem. Photobiol.* 58:895–900.
- Ehrenberg, B. 1992. Assessment of the partitioning of probes to membranes by spectroscopic titration. *J. Photochem. Photobiol. B. Biol.* 14:383–386.
- Ehrenberg, B., J. L. Anderson, and C. S. Foote. 1998. Kinetics and yield of singlet oxygen photosensitized by hypericin in organic and biological media. *Photochem. Photobiol.* 68:135–140.
- Ehrenberg, B., and E. Gross. 1988. The effect of liposomes' membrane composition on the binding of the photosensitizers HPD and Photofrin II. *Photochem. Photobiol.* 48:461–466.
- Ehrenberg, B., E. Gross, Y. Nitzan, and Z. Malik. 1993. Electric depolarization of photosensitized cells: lipid vs. protein alterations. *Biochim. Biophys. Acta.* 1151:257–264.
- Ehrenberg, B., Z. Malik, and Y. Nitzan. 1985. Fluorescent spectral changes of hematoporphyrin derivative upon binding to lipid vesicles. *S. aureus* and *E. coli* cells. *Photochem. Photobiol.* 41:429–435.
- Fischkoff, S., and J. M. Vanderkooi. 1975. Oxygen diffusion in biological and artificial membranes determined by the fluorochrome pyrene. *J. Gen. Physiol.* 65:663–676.
- Gomer, C. J. 1991. Preclinical examination of first and second generation photosensitizers used in photodynamic therapy. *Photochem. Photobiol.* 54:1093–1107.
- Gorman, A. A., and M. A. J. Rodgers. 1992. Current perspectives of singlet oxygen detection in biological environments. *J. Photochem. Photobiol. B. Biol.* 14:159–176.
- Gottfried, V., D. Peled, J. W. Winkelman, and S. Kimel. 1988. Photosensitizers in organized media: singlet oxygen production and spectral properties. *Photochem. Photobiol.* 48:157–163.
- Gross, E., and B. Ehrenberg. 1989. The partition and distribution of porphyrins in liposomal membranes. A spectroscopic study. *Biochim. Biophys. Acta.* 983:118–122.
- Gross, E., B. Ehrenberg, and F. M. Johnson. 1993. Singlet oxygen generation by porphyrins and the kinetics of 9,10-dimethylanthracene photosensitization in liposomes. *Photochem. Photobiol.* 57:808–813.
- Gross, E., Z. Malik, and B. Ehrenberg. 1987. Effects of membrane physical parameters on hematoporphyrin derivative binding to liposomes. A spectroscopic study. *J. Membr. Biol.* 97:215–221.
- Henderson, B. W., and T. J. Dougherty. 1992. How does photodynamic therapy work? *Photochem. Photobiol.* 55:145–157.
- Hoebeke, M., J. Piette, and A. Vandevorst. 1991. Photosensitized production of singlet oxygen by merocyanine 540 bound to liposomes. *J. Photochem. Photobiol. B. Biol.* 9:281–294.
- Holmes, R. T. 1997. Synthetic studies of poly-pyrrolic macrocycles. Ph.D. thesis. University of California, Davis.
- Kachel, K., E. Asuncion-Punzalan, and E. London. 1995. Anchoring of tryptophan and tyrosine analogs at the hydrocarbon polar boundary in model membrane vesicles: parallax analysis of fluorescence quenching induced by nitroxide-labeled phospholipids. *Biochemistry*. 34: 15475–15479.
- Kanofsky, J. R. 1989. Singlet oxygen production by biological systems. *Chem. Biol. Interact.* 70:1–28.
- Kennedy, J. C., and K. Oswald. 1984. HPD Photoradiation therapy in theory and in practice. In Porphyrins in Tumor Phototherapy. A. Andreoni and R. Cubeddu, editors. Plenum Press, New York. 365–374.
- Kessel, D. 1984. Hematoporphyrin and HPD: photophysics, photochemistry and phototherapy. *Photochem. Photobiol.* 39:851–859.
- Kessel, D., and E. Rossi. 1982. Determinants of porphyrin-sensitized photooxidation characterized by fluorescence and absorption spectra. *Photochem. Photobiol.* 35:37–41.
- Kusaj, S., P. Kaszycki, and Z. Wasylewski. 1996. A fluorescence quenching study on protoporphyrin IX in a model membrane system. *Chem. Phys. Lipids.* 83:153–160.
- Lam, S., E. C. Kostashuk, E. P. Coy, E. Laukkanen, J. C. LeRiche, H. A. Mueller, and I. J. Szasz. 1987. A randomized comparative study of the safety and efficacy of photodynamic therapy using Photofrin II combined with palliative radiotherapy versus palliative radiotherapy alone in patients with inoperable obstructive non-small cell bronchogenic carcinoma. *Photochem. Photobiol.* 46:893–897.
- Langner, M., and S. W. Hui. 1991. Iodide penetration into lipid bilayers as a probe of membrane lipid organization. *Chem. Phys. Lipids.* 60: 127–132.
- Lehrer, S. S. 1971. Solute perturbation of protein fluorescence. The quenching of the tryptophyl fluorescence of model compounds and of lysozyme by iodide ion. *Biochemistry*. 10:3254–3263.
- Li, J. H., Z. H. Guo, M. L. Jin, F. Y. Zhao, W. M. Cai, M. L. Gao, M. Y. Shu, and J. Zou. 1990. Photodynamic therapy in the treatment of malignant tumors: an analysis of 540 cases. *J. Photochem. Photobiol. B* 6:149–155.

- Malik, Z., and M. Djaldetti. 1980. Destruction of erythroleukemia, myelocytic leukemia and Burkitt lymphoma cells by photoactivated protoporphyrin. *Int. J. Cancer*. 26:495–500.
- McCaughan, J. S. 1987. Overview of experiences with photodynamic therapy for malignancy in 192 patients. *Photochem. Photobiol.* 46: 903–909.
- Moan, J., K. Berg, E. Kvam, A. Western, Z. Malik, A. Ruck, and H. Schneckenburger. 1989. Intracellular localization of photosensitizers. In *Photosensitizing Compounds: Their Chemistry, Biology and Clinical Use*. G. Bock and S. Harnett, editors. John Wiley and Sons, New York. 95–111.
- Moan, J., and K. Berg. 1992. Photochemotherapy of cancer-experimental research. *Photochem. Photobiol.* 55:931–948.
- Moretti, M. 1994. An eye for tomorrow's applications spells success in medical lasers. *Photonics Spectra*. 28:82–90.
- Moro, F., F. M. Goni, and M. A. Urbaneja. 1993. Fluorescence quenching at interfaces and the permeation of acrylamide and iodide across phospholipid bilayers. *FEBS Lett.* 330:129–132.
- Mulrone, C. M., S. Gluck, and A. D. Ho. 1994. The use of photodynamic therapy in bone marrow purging. *Semin. Oncol.* 21:24–27.
- North, J., H. Neyndorff, and J. G. Levy. 1993. Photosensitizers as virucidal agents. *J. Photochem. Photobiol. B. Biol.* 17:99–108.
- Paardekooper, M., P. J. Van den Broek, A. W. De Bruijne, J. G. Elferink, T. M. A. R. Dubbelman, and J. Van Steveninck. 1992. Photodynamic treatment of yeast cells with the dye toluidine blue: all-or-none loss of plasma membrane barrier properties. *Biochim. Biophys. Acta*. 1108: 86–90.
- Pandey, R. K., and G. Zheng. 2000. Porphyrins as photosensitizers in photodynamic therapy. In *The Porphyrin Handbook*, Vol. 6. K.M. Kadish, K.M. Smith, and R. Guillard, editors. Academic Press, Boston. Chapter 43, 157–230.
- Pottier, R., and T. G. Truscott. 1986. The photochemistry of haematoporphyrin and related systems. *Int. J. Radiat. Biol.* 50:421–452.
- Rodgers, M. A. J. 1988. On the problems involved detecting luminescence from singlet oxygen in biological specimens. *J. Photochem. Photobiol. B. Biol.* 1:371–373.
- Roslaniec, M., H. Weitman, D. Freeman, Y. Mazur, and B. Ehrenberg. 2000. Liposome binding constants and singlet oxygen quantum yields of hypericin, tetrahydroxy helianthone and their derivatives: studies in organic solutions and in liposomes. *J. Photochem. Photobiol. B. Biol.* 57:149–158.
- Schuitmaker, J. J., P. Bass, H. L. L. M. Van Leengoed, F. W. van der Meulen, W. M. Star, and N. Van Zandwijk. 1996. Photodynamic therapy: a promising new modality for the treatment of cancer. *J. Photochem. Photobiol. B. Biol.* 34:3–12.
- Shinitzky, M. 1979. The concept of passive modulation of membrane responses. *Dev. Cell. Biol.* 4:173–181.
- Shinitzky, M. 1984. *Physiology of Membrane Fluidity*. CRC Press, Boca Raton, FL.
- Shinitzky, M., and M. Inbar. 1976. Microviscosity parameters and protein mobility in biological membranes. *Biochem. Biophys. Acta*. 433: 133–149.
- Simon, S. A., T. J. McIntosh, and R. Lattore. 1982. Influence of cholesterol on water penetration into bilayers. *Science*. 216:65–67.
- Smith, K. M. 2000. Strategies for the Syntheses of Octaalkylporphyrin Systems. In *The Porphyrin Handbook*, Vol. 1. K.M. Kadish, K.M. Smith, and R. Guillard, editors. Academic Press, Boston. Chapter 1, 25–28.
- Specht, K. G., and M. A. J. Rodgers. 1991. Plasma membrane depolarization and calcium influx during cell injury by photodynamic action. *Biochim. Biophys. Acta*. 1070:60–68.
- Straight, R. C., and J. D. Spikes. 1985. Photosensitized oxidation of biomolecules. In *Singlet O<sub>2</sub>*. A. A. Frimer, editor. CRC Press, Boca Raton. 91–143.
- Usui, Y. 1973. Determination of quantum yield of singlet oxygen formation by photosensitization. *Chem. Lett.* 743–744.
- Van der Meer, B. W. 1993. Fluidity, dynamics and order. In *Biomembranes, Physical Aspects*. M. Shinitzky, editor. VCH, Weinheim, Germany. 97–158.
- Van Hillegersberg, R., W. J. Kort, and J. H. P. Wilson. 1994. Current status of photodynamic therapy in oncology. *Drugs*. 48:510–527.
- Wasserman, H. A., and R. W. Murray. 1979. *Singlet Oxygen*. Academic Press, NY.
- Wilkinson, F., and J. Brummer. 1981. Rate constants for the decay and reactions of the lowest electronically excited singlet state of molecular oxygen in solution. *J. Phys. Chem. Ref. Data*. 10:809–999.
- Wilkinson, F., W. P. Helman, and A. B. Ross. 1995. Rate constants for the decay and reactions of the lowest electronically excited singlet state of molecular oxygen in solution. an expanded and revised compilation. *J. Phys. Chem. Ref. Data*. 24:663–1021.
- Zavoico, G. B., L. Chandler, and H. Kutchai. 1985. Perturbation of egg phosphatidylcholine and dipalmitoylphosphatidylcholine multilamellar vesicles by *n* alkanols. A fluorescent probe study. *Biochem. Biophys. Acta* 812:299–312.